General Theory and Design of Optimum Quarter-Wave TEM Filters

M. C. HORTON, MEMBER, IEEE, AND R. J. WENZEL, MEMBER, IEEE

Abstract—The exact synthesis and design of a broad class of quarter-wave TEM mode filters is presented in a three-step procedure. The theory is applicable to all microwave filter forms consisting entirely of a cascade of quarter-wave lines, quarter-wave stubs, and coupled quarter-wave lines. The exact design of many conventional filter forms that heretofore could only be designed using approximate methods is possible using the techniques and functions described. General approximating functions that give the "best" transmission response in a Butterworth or Chebyshev sense are derived. The use of a maximum number of available singularities to augment the filter skirt response leads to a minimum element filter termed "optimum multipole." An optimum multipole design insures the "best" possible response for the minimum element and all corresponding redundant element networks. The designer has the freedom of introducing sufficient redundancy to obtain a design that is practical to construct, but which still realizes the optimum response. Judicious choice of network form often results in improved performance and reduced size in comparison with many conventional filter forms. Design procedures are presented that allow the practical realization of distributed filter networks in the form of quarter-wave lines. A design example and experimental results are given to confirm the theory.

I. Introduction

PREVIOUS TEM distributed filter designs have made use of either approximate image parameter techniques [1]–[3] or exact modern network techniques [4]–[12]. The modern network approach allows the realization of prescribed transfer characteristics at all frequencies and is, therefore, preferred, especially for wide-band-pass or band-stop responses of 30 per cent or greater. However, in the exact design approach, quarter-wave unit elements often serve only to spatially separate adjacent distributed stub-type elements so their fields do not interact. In most designs of this type, no use has been made of the unit elements to help in achieving a desired maximally flat or equal ripple response. Other microwave filter forms, previously designed by approximate methods, depend almost entirely on the unit element "spacers" to obtain a useful response. A method was sought for obtaining an exact procedure which would permit an optimum design in each of these important cases.

This paper presents the theory and design of a broad class of TEM filters employing commensurate length lines. The theory includes all microwave filter forms consisting entirely of a cascade of quarter-wave lines, quarter-wave stubs, and coupled quarter-wave lines. A filter form termed "optimum multipole" is obtained when each line length element characterized in the theory is used to create a complex plane pole to augment the filter skirt response. Most conventional network forms are obtained from the optimum multipole form by introducing redundant elements.

Throughout the paper a heuristic understanding is stressed at the possible expense of mathematical rigor. An outline is given for the steps employed in the synthesis of distributed TEM filters; however, many details of modern network synthesis are beyond the scope of this paper and may be reviewed in existing publications [13]–[15].

II. TEM Distributed Networks

The application of modern network theory to the design of microwave TEM distributed networks is based upon a complex plane transformation demonstrated by Richards [16] in 1948. He showed that distributed networks, composed of commensurate lengths of transmission line and lumped resistors, could be treated in analysis or synthesis as lumped L-C-R networks by using the complex frequency variable

$$S = j\Omega = j \tan \frac{\pi\omega}{2\omega_0} \tag{1}$$

where Ω is real and ω_0 is the radian frequency for which the transmission lines are a quarter wavelength. The tangent mapping function converts the range of frequencies $-\omega_0 \leq \omega \leq \omega_0$ into the range $-\infty \leq \Omega \leq \infty$ and the mapping is repetitious in increments of $2\omega_0$. For example, the high-pass response of a lumped element filter in the frequency variable Ω maps into a band-pass response in ω about the quarter-wave frequency ω_0 for the corresponding distributed filter, as shown in Fig. 1.

The one-port impedance of a short-circuited transmission line

$$Z = \left(j \tan \frac{\pi\omega}{2\omega_0}\right) Z_{0L}$$

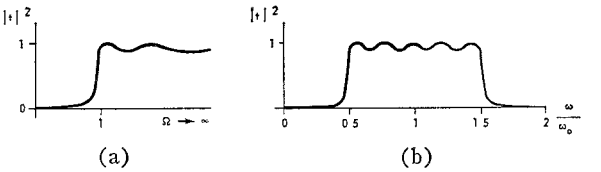

(a) (b)

Fig. 1. Mapping properties of the transformation $\Omega = \tan \pi\omega/2\omega_0$. (a) Prototype lumped element high-pass. (b) Corresponding distributed element band-pass.

Manuscript received September 8, 1964; revised January 22, 1965.
The authors are with Research Laboratories Div., The Bendix Corp., Southfield, Mich.

corresponds in the mapping transformation to the impedance of a lumped inductor, $Z=j\omega L$. Similarly, the admittance of an open-circuit line

$$Y = \left(j \tan \frac{\pi\omega}{2\omega_0}\right) Y_{0_C}$$

corresponds to the admittance of a lumped capacitor $Y=j\omega C$. The distributed characteristic values of Z_{0_L} and Y_{0_C} correspond, respectively, to L and C for lumped elements. Throughout the remainder of this paper, the symbols L (inductor) and C (capacitor) will be used to designate the characteristic impedance or admittance of a short-circuited or open-circuited quarter-wave line, respectively.

The application of exact synthesis methods to microwave networks using the transformation of (1) is reviewed in detail by Wenzel [4]. The "unit element" (u.e.), a quarter-wave two-port transmission line of characteristic impedance Z is introduced as a network element which has no identical counterpart in lumped element theory. Kuroda's Identities [4], [5], [17] are also introduced to enable the interchange of cascaded u.e.'s with series or shunt distributed L's or C's.

III. The Optimum Multipole Filter

An optimum multipole filter is defined as a nonredundant two-port network constructed of elements whose values have been chosen to yield the best approximation to a rectangular transfer response in a Butterworth or Chebyshev sense. A nonredundant network is one in which each element contributes a complex plane pole that can be used to augment the filter skirt response. Every nonredundant combination of quarter-wave stubs (LC elements) and unit elements can be used to obtain an optimum multipole filter. All filters employing only quarter-wave lines can be reduced to nonredundant form by suitable application of Kuroda's Identities and/or series parallel reduction. It is obvious that the introduction of redundant elements cannot lead to a network form whose response is better than that of the corresponding optimum multipole filter.

As a specific example of the application of the previous statements to a network containing unit elements, consider the familiar parallel coupled band-pass filter. The conventional form consists of a cascade of series capacitors and unit elements. A filter with K series capacitors and N unit elements can be reduced to a nonredundant form having one series capacitor and N unit elements [4]. (This assumes that none of the u.e.'s are redundant.) Assignment of element values in accordance with the theory to be described gives an optimum multipole design and insures the best possible response for the minimum element network and for any redundant element network derived therefrom. The designer now has the freedom of introducing just enough redundancy to obtain a filter that is practical to construct but which realizes the optimum multipole response. In fact, a practical redundant network can often be obtained directly from the synthesis procedure, especially if a specific network realization is desired.[1]

IV. Design of Optimum Distributed Filters

The exact design of microwave TEM distributed filters based on modern network theory involves three distinct steps:

1) Determination of the polynomial form of the ratio of reflection to transmission coefficient for a composite two-port filter containing both quarter-wave short or open-circuited stubs (LC's) and quarter-wave impedance transforming two-ports (u.e.'s).
2) Development of the approximating function, usually chosen as maximally flat (Butterworth) or equal ripple (Chebyshev), used to approximate a rectangular low-pass or high-pass prototype power transmission characteristic.
3) Synthesis and physical realization of a practical network in the form of distributed quarter-wave lines.

A. Step 1—Polynomial Ratio of Reflected to Transmitted Power

The polynomial ratio of reflection to transmission coefficient for a cascade of unit elements and prototype LC distributed elements can be obtained by multiplication of wave cascading matrices R [18] defined by

$$\begin{bmatrix} b_1 \\ a_1 \end{bmatrix} = \begin{bmatrix} r_{11} & r_{12} \\ r_{21} & r_{22} \end{bmatrix} \begin{bmatrix} a_2 \\ b_2 \end{bmatrix} = \frac{1}{s_{21}} \begin{bmatrix} -\Delta_s & s_{11} \\ -s_{22} & 1 \end{bmatrix} \begin{bmatrix} a_2 \\ b_2 \end{bmatrix}. \tag{2}$$

In this equation a_1, b_1, are the left-hand port incident and reflected wave amplitudes, respectively, and a_2, b_2 are those of the right-hand port. The r_{ij}'s are the R-matrix elements, the s_{ij}'s are the scattering S-matrix elements, and $\Delta_s = s_{11}s_{22} - s_{12}s_{21}$ is the scattering matrix determinant. The individual R-matrices of cascaded two-ports can be multiplied to give the overall R-matrix of the cascade.

The constant matrix A with transpose $\tilde{A}$, is defined by

$$A = \frac{1}{2} \begin{bmatrix} -1 & -1 \\ 1 & 1 \end{bmatrix} \tag{3}$$

and appears in the R-matrix for each of the distributed L's, C's and u.e.'s of Table I.

1) *High-pass prototype:* The high-pass prototype response, which, as shown in Fig. 1, gives rise to a distributed filter band-pass response, will be considered

[1] See, for example, Wenzel [4], pp 109–110. The first synthesis procedure described gives an optimum multipole network, while the second yields a redundant form in which all unit elements were chosen to have unity characterisic impedance. Depending on the element values, one form may be more suitable than the other from a practical viewpoint.

TABLE I

WAVE CASCADE MATRIX, R, FOR DISTRIBUTED LC LADDER AND UNIT ELEMENTS. THE CONSTANT MATRIX, A, IS DEFINED IN (3), AND I IS THE IDENTITY MATRIX

FILTER ELEMENTS		SCHEMATIC	R-MATRIX
LOW PASS	L		$LS\left(\frac{1}{LS}\ I+\tilde{A}\right)$
	C		$CS\left(\frac{1}{CS}\ I+A\right)$
	u.e		$\frac{S}{\sqrt{1-S^2}}\left[\frac{1}{S}\ I+(Z\tilde{A}+Z^{-1}A)\right]$
HIGH PASS	u.e		$\frac{1}{\sqrt{1-S^2}}\left[(Z\tilde{A}+Z^{-1}A)\ S+I\right]$
	C		$\frac{1}{CS}\ (CS\ I+\tilde{A})$
	L		$\frac{1}{LS}\ (LS\ I+A)$

first. Such a filter may be comprised of distributed series C's, shunt L's, u.e.'s, and a unit terminating load. The C's, L's, and u.e.'s may occur in random sequence; however, in order to be a nonredundant filter, no two C's nor two L's may occur adjacent to each other even if separated by one or more u.e.'s.[2] It is noted in Table I that each of the lossless high-pass elements (C's, L's, u.e.'s) has an R-matrix which comprises a scalar denominator factor multiplied by a matrix which is linear in the frequency parameter S. The scalar denominator factor of each R-matrix contains S to the first order. Thus, an optimum high-pass filter, having a mixed cascade of m high-pass ladder elements and n unit elements terminated in a unit load, will have an overall R-matrix of the form

$$R = \left(\frac{1}{S}\right)^m \left(\frac{1}{\sqrt{1-S^2}}\right)^n B_{m+n}(S) \tag{4}$$

where $B_{m+n}(S)$ is an $(m+n)$th degree 2×2 matrix polynomial in S,

$$B_{m+n}(S) = \begin{bmatrix} b_{11}(S) & b_{12}(S) \\ b_{21}(S) & b_{22}(S) \end{bmatrix}_{m+n}. \tag{5}$$

The R-matrix element of interest in (2) is $r_{12}=s_{11}/s_{21}$ representing the ratio of input reflected wave to that transmitted into the load.

$$r_{12} = s_{11}/s_{21} = \left(\frac{1}{S}\right)^m \left(\frac{1}{\sqrt{1-S^2}}\right)^n b_{12m+n}(S). \tag{6}$$

The overall cascade input reflection coefficient $\rho=s_{11}$ and the transmission coefficient into the unit load $t=s_{21}$ are now renamed for ease in recognition. Total power into the filter is conserved, thus

$$|\rho|^2 + |t|^2 = 1 \tag{7}$$

which can be rearranged to show the dependence of the power transmission response on $r_{12}=\rho/t$, i.e.,

$$|t|^2 = \frac{1}{1+|\rho|^2/|t|^2} = \frac{1}{1+|r_{12}|^2}. \tag{8}$$

Equation (6) for $r_{12}(S)$, when multiplied by $r_{12}(-S)$ to give $|r_{12}|^2$, results in a ratio of $(m+n)$th degree polynomials in $(-S^2)$. The general form of the resultant numerator polynomial, which has real coefficients, will not change if each term is multiplied by a real constant involving $S_c^2=(j\tan\theta_c)^2$, where $\theta_c=\pi\omega_c/2\omega_0$ and ω_c is designated to be the filter cutoff frequency. Then

$$\frac{|\rho|^2}{|t|^2} = \left(\frac{-S_c^2}{-S^2}\right)^m \left(\frac{1-S_c^2}{1-S^2}\right)^n P_{m+n}\left(\frac{-S^2}{-S_c^2}\right) \tag{9}$$

or from (1),

$$\frac{|\rho|^2}{|t|^2} = \left(\frac{\tan\theta_c}{\tan\theta}\right)^{2m} \left(\frac{\cos\theta}{\cos\theta_c}\right)^{2n} P_{m+n}\left(\frac{\tan^2\theta}{\tan^2\theta_c}\right) \tag{10}$$

where P_{m+n} is an $(m+n)$th degree polynomial in $-S^2/-S_c^2$.

2) *Low-pass prototype:* The individual R-matrices of an optimum low-pass (L-P) filter having m low-pass ladder elements, n unit elements, and a unit termination, may be multiplied to obtain the overall R-matrix of the cascade. The low-pass optimum filter may be comprised of series L's, shunt C's and u.e.'s in random sequence; however, to be nonredundant, L's must be adjacent to C's if not separated by a u.e., or L's must be adjacent to each other (and likewise C's) if separated by a u.e.

By applying a procedure similar to that used above for the high-pass filter, the low-pass prototype response ratio of reflected to transmitted power is given by:

$$\frac{|\rho|^2}{|t|^2} = \left(\frac{-S^2}{-S_c^2}\right)^m \left(\frac{-S^2(1-S_c^2)}{-S_c^2(1-S^2)}\right) Q_{m+n}\left(\frac{-S_c^2}{-S^2}\right) \tag{11}$$

or by

$$\frac{|\rho|^2}{|t|^2} = \left(\frac{\tan\theta}{\tan\theta_c}\right)^{2m} \left(\frac{\sin\theta}{\sin\theta_c}\right)^{2n} Q_{m+n}\left(\frac{\tan^2\theta_c}{\tan^2\theta}\right) \tag{12}$$

where Q_{m+n} is an $(m+n)$th degree polynomial in $(-S_c^2/-S^2)$.

B. Step 2—Approximating Functions

The ideal microwave prototype filter has a transmission power-amplitude response, (8), which is rectangular; i.e., as frequency increases through cutoff, it is desired that transmission $|t|^2$ change from zero to unity for a high-pass prototype and from unity to zero for a low-pass prototype, as shown in Fig. 2.

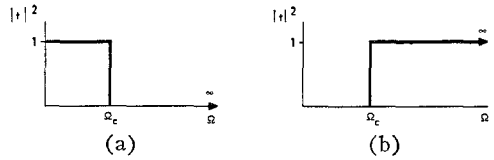

Fig. 2. Ideal rectangular transmission amplitude power response. (a) L-P prototpye. (b) H-P prototype.

[2] Otherwise the elements may be combined, reducing the total number, by simple parallel or series combinations possibly in conjunction with use of one of Kuroda's Identities.

This rectangular response cannot be realized exactly and, therefore, must be approximated in some manner. The two most common approximations, which are considered here for application to the optimum multipole filter are the maximally flat (Butterworth) and the equal ripple (Chebyshev).

1) *Butterworth:* The maximally flat approximation for the high-pass prototype results from choosing coefficients of the $(m+n)$th degree polynomial P_{m+n} (9) in a manner such that all but the highest order derivative of $|\rho|^2/|t|^2$, taken with respect to S^{-1}, are zero at $S^{-1}=0$ $(S=\infty)$. This criterion requires that all coefficients in P_{m+n} be zero except the constant term. A constant term of unity defines the cutoff frequency $\Omega_c=S_c/j$ to occur at half power (-3 dB) as verified by inspection of (8) and (9).

Similarly, all coefficients of Q_{m+n} (11) are set equal to zero, except the constant coefficient of unity, to obtain the low-pass maximally flat approximation. In the low-pass case, all but the highest order derivative of $|\rho|^2/|t|^2$, taken with respect to S, are zero at $S=0$.

The Butterworth approximating functions are then given by:

$$\text{H-P:}\quad \frac{|\rho|^2}{|t|^2}=\left(\frac{S_c}{S}\right)^{2m}\left(\frac{\sqrt{1-S_c^2}}{\sqrt{1-S^2}}\right)^{2n}=\left(\frac{\tan\theta_c}{\tan\theta}\right)^{2m}\left(\frac{\cos\theta}{\cos\theta_c}\right)^{2n}$$

$$\text{L-P:}\quad \frac{|\rho|^2}{|t|^2}=\left(\frac{S}{S_c}\right)^{2m}\left(\frac{S\sqrt{1-S_c^2}}{S_c\sqrt{1-S^2}}\right)^{2n}=\left(\frac{\tan\theta}{\tan\theta_c}\right)^{2m}\left(\frac{\sin\theta}{\sin\theta_c}\right)^{2n}. \tag{13}$$

Note that the low-pass approximation can be obtained directly from the high-pass by replacing each frequency parameter (i.e., S, S_c) by its respective inverse (S^{-1}, S_c^{-1}), and vice versa.

2) *Chebyshev:* An equal ripple approximation for the high-pass prototype results from choosing coefficients of the polynomial, P_{m+n} (9), in such a manner that the pass band response ripples between the values of unity and $(1+\epsilon^2)^{-1}$. The polynomial form which exhibits this response is developed (see Appendix) from a constant amplitude rational fraction all-pass function.

This same development, with each frequency parameter replaced by its inverse, gives the proper coefficients of Q_{m+n} (11) for equal ripple pass band response of the low-pass prototype.

The Chebyshev approximating functions are given by:

$$\text{H-P:}\quad \frac{|\rho|^2}{|t|^2}=\epsilon^2\left[T_m\left(\frac{S_c}{S}\right)T_n\left(\frac{\sqrt{1-S_c^2}}{\sqrt{1-S^2}}\right)-U_m\left(\frac{S_c}{S}\right)U_n\left(\frac{\sqrt{1-S_c^2}}{\sqrt{1-S^2}}\right)\right]^2$$
$$=\epsilon^2\left[T_m\left(\frac{\tan\theta_c}{\tan\theta}\right)T_n\left(\frac{\cos\theta}{\cos\theta_c}\right)-U_m\left(\frac{\tan\theta_c}{\tan\theta}\right)U_n\left(\frac{\cos\theta}{\cos\theta_c}\right)\right]^2$$

$$\text{L-P:}\quad \frac{|\rho|^2}{|t|^2}=\epsilon^2\left[T_m\left(\frac{S}{S_c}\right)T_n\left(\frac{S\sqrt{1-S_c^2}}{S_c\sqrt{1-S^2}}\right)-U_m\left(\frac{S}{S_c}\right)U_n\left(\frac{S\sqrt{1-S_c^2}}{S_c\sqrt{1-S^2}}\right)\right]^2$$
$$=\epsilon^2\left[T_m\left(\frac{\tan\theta}{\tan\theta_c}\right)T_n\left(\frac{\sin\theta}{\sin\theta_c}\right)-U_m\left(\frac{\tan\theta}{\tan\theta_c}\right)U_n\left(\frac{\sin\theta}{\sin\theta_c}\right)\right]^2 \tag{14}$$

where

$T_m(x)=\cos(m\arccos x)$ and $U_m(x)=\sin(m\arccos x)$

are unnormalized mth degree Chebyshev polynomials of the first and second kinds, respectively [19].

C. Step 3—Network Synthesis

The final step in obtaining an optimum filter is solving the realization problem; i.e., it is desired to synthesize a distributed network with a physical response corresponding to the admissible approximating function of (13) or (14). The general form of these functions was obtained by considering a cascade of unit elements and distributed L's and C's. If the input impedance of this cascade is determined from the specified power function, Richards' Theorem[3] can be applied to determine the unit element values, and pole removing techniques [13]–[15] can be used to determine the LC values. The power reflection coefficient $|\rho|^2=1-|t|^2=\rho\bar{\rho}$ where the bar denotes complex conjugate, can be obtained from the approximating function for $|\rho|^2/|t|^2$. Because the network is to be physically realizable, the reflection coefficient ρ must have no poles in the right half plane. Since the network functions under consideration do not have j-axis poles, the desired reflection coefficient can be determined from the squared approximating function $|\rho|^2$ by finding roots of the numerator and denominator polynomials and associating the left half-plane poles with ρ and the right half-plane poles with $\bar{\rho}$. The only restriction on the zeros of ρ is that they be chosen in conjugate pairs such that the numerator of $\rho\bar{\rho}$ is the numerator of $|\rho|^2$.[4] For many practical microwave filters, all zeros lie on the imaginary axis and no alternate choices are possible.

[3] For a statement and discussion of Richard's Theorem see [4], [5], [6], [8], and [16].

[4] For a discussion of the effects of different zero distributions, see Weinberg [14], pp 592–595.

Once a reflection coefficient has been obtained by the above procedure, the transformation

$$Z_{in} = \frac{1+\rho}{1-\rho} \tag{15}$$

yields the input impedance of one possible network and the opposite choice for the algebraic sign of ρ gives the input impedance of the dual network. The choice of either network is dictated by the physical configuration of the desired realization and the element values obtained from the synthesis procedure.

Many variations in network form, each having a minimum number of elements, are possible. Specifically, there exists a number of configurations equal to the number of unique networks that can be obtained by applying Kuroda's Identities. Furthermore, redundancy (for example, replacing a series inductor by two inductors or adding u.e.'s whose impedance is the same as that of the load) allows the possibility of additional network forms. Any one of the minimum element networks is a permissible mathematical solution; however, a practical realization may require that various network forms be investigated.

The schematic forms of two symmetric, doubly terminated, optimum filters and their respective duals are shown in Table II. The forms shown utilize the maximum number of elements that can usually be obtained in a practical network.

In some specific cases, series elements can be contained within shunt stubs, and multiple stubs can be contained within u.e.'s, thereby increasing filter complexity for a given number of unit elements. In general, this can be accomplished only in relatively wide-band designs and at lower microwave frequencies where element value restrictions and complicated junctions do not present serious limitations. Symmetry in the assumed forms requires equal terminating impedances; however, for the band-pass case, Kuroda's Identities often can be applied to provide for unequal terminations. In general, the filters need not be symmetric and all combinations of m and n may be used. The networks shown in Table II can be used as a guide in applying Richards' Theorem and pole removing techniques to Z_{in}, together with application of Kuroda's Identities, to obtain equivalent forms. Because of the assumed symmetry, only part of each network need be synthesized. For example, in the symmetrical case of five ladder elements ($m=5$) and two unit elements ($n=2$), the network is synthesized by applying Richards' Theorem once to obtain the unit element value followed by three pole removals.

It is evident that an optimum filter can contain many sections in a relatively short overall length. In some applications, use of the full number of sections possible in a given length may not be necessary or practical. For example, networks having two u.e.'s can contain up to five LC elements (not including the possibility of series stubs within shunt elements and multiple stubs in u.e.'s). The use of fewer LC elements or redundancy may in some cases simplify the construction of the filter and may also ease the element value requirements. Several common filter forms that contain fewer than a maximum number of elements, or redundant elements, are listed in Table III. Networks of this type with optimum response can be exactly synthesized by using the appropriate m and n in (13) or (14).

TABLE II

EXAMPLES OF PRACTICAL OPTIMUM MULTIPOLE FILTER NETWORKS AND THEIR RESPECTIVE DUALS

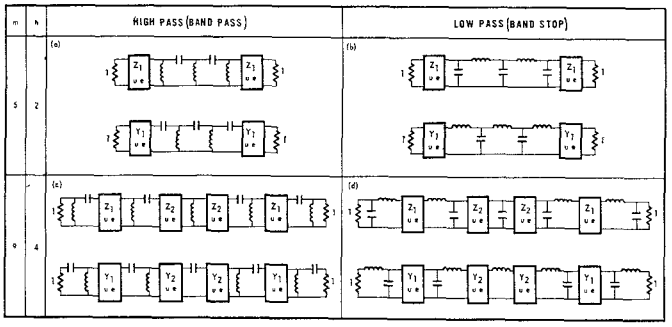

TABLE III

SOME COMMON FILTER FORMS CONTAINING FEWER THAN MAXIMUM ELEMENTS OR REDUNDANT ELEMENTS THAT CAN BE EXACTLY DESIGNED TO GIVE AN OPTIMUM MULTIPOLE RESPONSE BY SUITABLE CHOICE OF m AND n

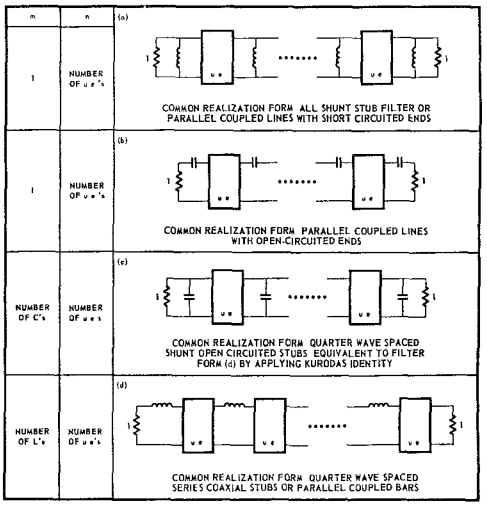

Bandwidth scaling of optimum filter network element values is not as easily accomplished as it is in networks incorporating only ladder elements. For networks that have a ladder prototype, a set of normalized element values can be determined and bandwidth renormalization may be accomplished by multiplying these values by a constant. Variation of the bandwidth determining constant (S_c) for the general optimum filter changes the element values in a manner which may not permit a simple calculation to yield the new values. A digital computer, however, can be used to obtain tables of element values for a wide range of bandwidths.

The manner in which prototype element values are converted to physical dimensions and a general discussion of equivalent network forms can be found in the literature [4], [5], [6], [9], [12].

V. Experimental Evaluation

A seven-section equal ripple band-pass filter of 3 to 1 bandwidth[5] will be considered in detail as a design example. The filter, consisting of two unit elements and five LC elements, will be designed to have 0.1 dB ripple in the pass band. The normalized cutoff frequency for a 3 to 1 band is $S_c=j$. From (8) and (14) the transmission function is given by:

$$|t|^2 = \frac{1}{1+0.0233\left[T_5\left(\frac{S_c}{S}\right)T_2\left(\frac{\sqrt{1-S_c^2}}{\sqrt{1-S^2}}\right) - U_5\left(\frac{S_c}{S}\right)U_2\left(\frac{\sqrt{1-S_c^2}}{\sqrt{1-S^2}}\right)\right]^2}. \tag{16}$$

Substitution of $S_c=j$, simplification of the resultant ratio of polynomials, and use of the identity $|\rho|^2+|t|^2=1$ gives:

$$|\rho|^2 = \frac{[0.98S^6 + 8.15S^4 + 17.64S^2 + 10.78]^2}{-S^{14} + 2.96S^{12} + 14.96S^{10} + 100.96S^8 + 308.69S^6 + 487.06S^4 + 380.46S^2 + 116.23}. \tag{17}$$

Roots of the denominator are obtained with the use of a computer and the left-hand plane poles are associated with ρ. Since the numerator of $|\rho|^2$ is a perfect square, the numerator of ρ is obtainable by inspection:

$$\rho = -\frac{0.98S^6 + 8.15S^4 + 17.64S^2 + 10.78}{S^7 + 6.16S^6 + 17.47S^5 + 32.36S^4 + 39.13S^3 + 37.57S^2 + 20.73S + 10.78}. \tag{18}$$

Use of the linear transformation $Z_{in}=(1+\rho)/(1-\rho)$ yields

$$Z_{in} = \frac{S^7 + 5.18S^6 + 17.47S^5 + 24.21S^4 + 39.13S^3 + 19.93S^2 + 20.73S}{S^7 + 7.13S^6 + 17.47S^5 + 40.51S^4 + 39.13S^3 + 55.21S^2 + 20.73S + 21.56}. \tag{19}$$

One possible network form is shown in Table II(a). Determination of element values begins with the removal of a unit element by application of Richards' Theorem to give $Z_{u.e.}=Z_{in}(1)=0.63$. The impedance of the remaining network after removal of the u.e. is:

$$Z_{in}'(S) = Z_{in}(1)\frac{SZ_{in}(1) - Z_{in}(S)}{SZ_{in}(S) - Z_{in}(1)}$$

or

$$Z_{in}'(S) = \frac{1.84S^6 + 10.20S^5 + 18.84S^4 + 33.65S^3 + 20.08S^2 + 20.98S}{4.64S^6 + 21.09S^5 + 64.83S^4 + 82.37S^3 + 128.05S^2 + 60.52S + 62.96} \tag{20}$$

after cancellation of the common S^2-1 factor.

Next, a shunt inductor of value $L_1=0.33$ is removed by dividing the numerator of $Y_{in}'(S)=1/Z_{in}'(S)$ by its denominator.[6] A series capacitor of value $C=1.27$ and a shunt inductor of value $L_2=0.26$ are obtained from the impedance of the remaining network,

$$Z_{in}''(S) = \frac{5.54S^5 + 30.73S^4 + 56.77S^3 + 101.42S^2 + 60.52S + 62.96}{13.98S^5 + 46.87S^4 + 102.76S^3 + 77.15S^2 + 80.25S} \tag{21}$$

[5] As with conventional Chebyshev-type characteristics, the bandwidth is measured between the outer ripple points.

[6] This step removes a simple pole of Y_{in} at $S=0$ and is the same technique that is used to synthesize lumped element ladder networks [13]–[15].

in a similar manner. A diagram of the synthesis steps, together with the completely synthesized network, is shown in Fig. 3.

In order to obtain a network configuration that is convenient to construct, the following Kuroda Identity transformations are performed. Referring to Fig. 4, the 0.33 ohm distributed inductors and 1.27 mho distributed capacitors are transformed to the outside of the unit elements. Because the network is symmetric, the transformers can be moved to the center of the network and eliminated as in Fig. 4(c) [4]. The network of Fig. 4(c) contains a minimum number of elements and is still in optimum multipole form.[7] However, the center inductor value is low, requiring a 5.15 ohm shunt stub in a 50 ohm terminated filter realization. Two parallel 10.3 ohm stubs could be used, one on either side of the center line, but these values are still low to realize easily. To obtain more convenient center element values, redundant elements are introduced by splitting the center inductor into three inductors. The three element values are chosen such that application of Kuroda's Identity and elimination of the resulting transformers gives element values that do not differ greatly from the characteristic impedance of the terminations. The final network is shown in Fig. 4(f). The introduction of redundant elements in the manner described has yielded a network with realizable element values, but has not resulted in increasing the filter length. The final filter is not in optimum multipole form, but it does realize the optimum response for $m=5$ and $n=2$.

A trial filter was constructed based on the parameters used in the design example. A ground plane spacing of 0.200 inch was chosen and center conductor rod dimensions were obtained with the aid of standard graphs [20]. The unit elements were made one-quarter wavelength long at 2.175 Gc. Stub lengths were determined experimentally by adjusting each to produce a zero of transmission at 4.350 Gc by temporarily shortening all other stubs. A line drawing of the entire filter is shown in Fig. 5 and a photograph is shown in Fig. 6. To reduce undesirable junction effects, the two outer junctions were mitered as shown in Fig. 5. When first constructed, the bandwidth of the filter was about one per cent too narrow and the center frequency was about two per cent low. Slight adjustment of the shunt stub lengths resulted in a measured response that agrees very closely with the theoretical characteristics. Both theoretical and experimental curves are shown in Fig. 7. Note especially the measured VSWR vs. frequency which contains seven ripples commensurate with the five ladder elements and two unit elements incorporated in the design.

[7] This form can be obtained directly from (19) without the aid of Kuroda's Identities by removing a shunt inductor, series capacitor, unit element, and shunt inductor using the synthesis techniques described.

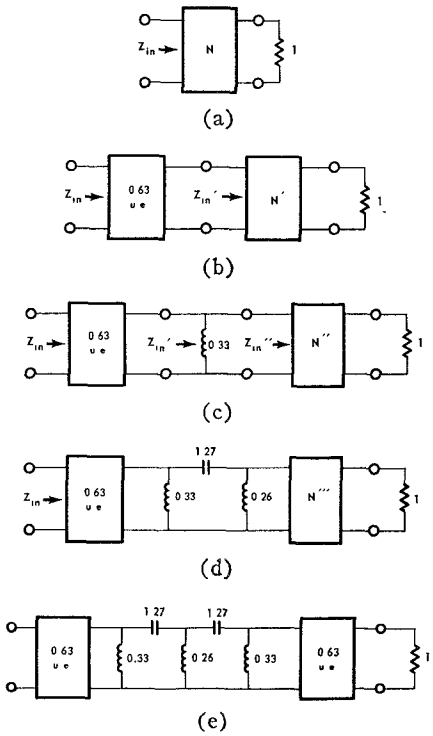

Fig. 3. Synthesis steps in seven-section filter design example. (a) Unsynthesized network. (b) Removal of a unit element by use of Richards' Theorem. (c) Removal of a shunt stub by removing a pole of $Y_{in}'(S)$ at $S=0$. (d) Removal of two more stubs in a manner similar to (c). (e) Final network obtained by symmetry.

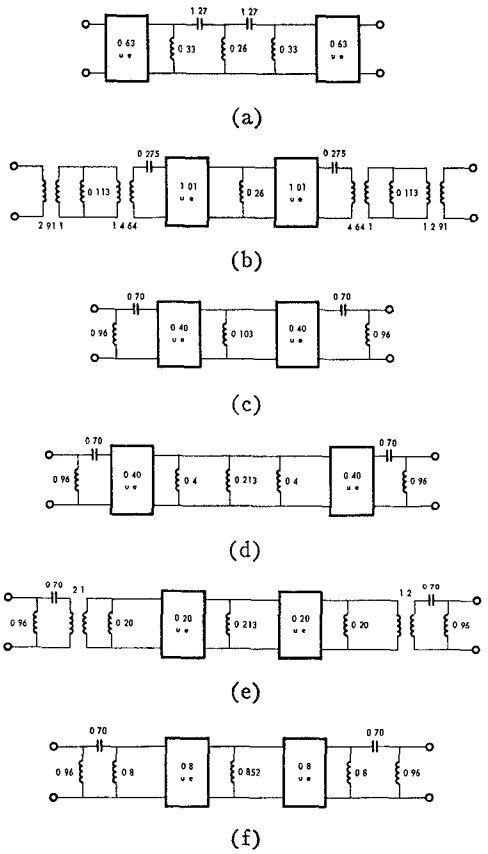

Fig. 4. Application of Kuroda's Identities to obtain convenient element values. (a) Initial prototype network. (b) Transformation of 0.33 ohm distributed inductors and 1.27 mho distributed capacitors. (c) Elimination of transformers. (d) Introduction of redundant elements. (e) Application of Kuroda's Identity. (f) Final network after elimination of transformers.

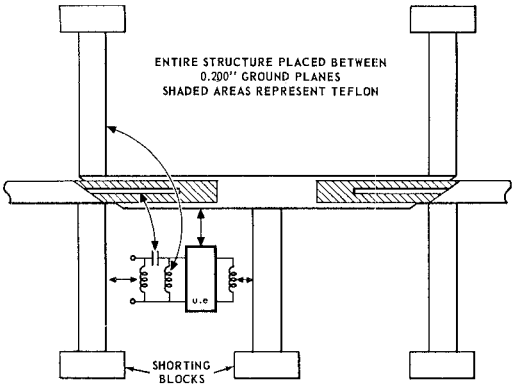

Fig. 5. Detailed view of an experimental filter that realizes a seven-section filter ($m=5$, $n=2$).

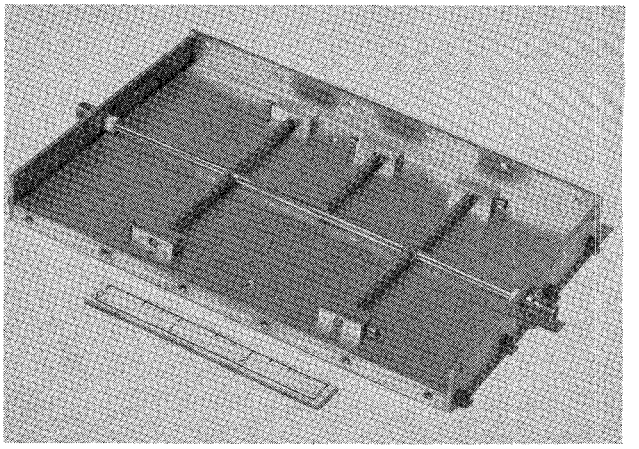

Fig. 6. Experimental seven-section filter ($m=5$, $n=2$).

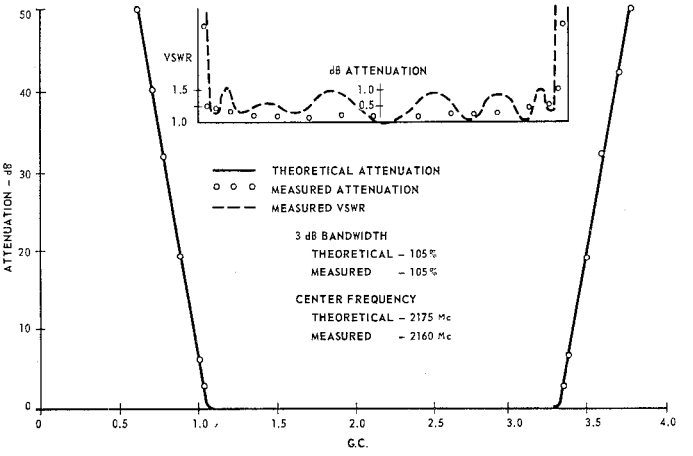

Fig. 7. Theoretical and experimental response characteristics of a seven-section filter ($m=5$, $n=2$).

VI. Comparison of Optimum Filter Networks

The optimum response of a filter network with a given number of nonredundant elements is obtained by use of (8) and (13) or (14). Given k nonredundant elements, m and n can be chosen in any manner such that $m+n=k$, and each choice will result in an optimum multipole filter of order k. The response of each network will be different, and the relation of one response to another will change with filter bandwidth. In narrow-band cases, practical considerations dictate the manner in which m and n should be chosen whereas for wide-band filters size considerations are of most importance.

Optimum multipole filter responses can be compared by investigating the filtering properties of unit elements in comparison with LC-type elements. The following comparison will be carried out for the Chebyshev high-pass prototype (band-pass filter) with the results for the low-pass case being obtained by the high-pass to low-pass transformation. Similar results apply for the Butterworth case. For convenient calculation of stop-band attenuation, (14) is written as:

$$\frac{|\rho|^2}{|t|^2} = \epsilon^2 \cosh^2\left[m \cosh^{-1}\frac{\Omega_c}{\Omega} + n \cosh^{-1}\frac{\sqrt{1+\Omega_c^2}}{\sqrt{1+\Omega^2}}\right] \quad \text{when } \Omega < \Omega_c. \quad (22)$$

This form follows from (35) and (36) of the Appendix, together with (1), using the identities $\cos^{-1} x = j \cosh^{-1} x$ and $\cos jx = \cosh x$. If n is zero, the function corresponds to the response of an LC ladder prototype and available nomographs [21] can be used to obtain the network response. The general optimum multipole function (22) can be adapted for use with these nomographs in the following manner. Inspection of the functions $\cosh^{-1} \Omega_c/\Omega$ and $\cosh^{-1} (\sqrt{1+\Omega_c^2}/\sqrt{1+\Omega^2})$ shows that the ratio

$$R = \frac{\cosh^{-1}\dfrac{\Omega_c}{\Omega}}{\cosh^{-1}\dfrac{\sqrt{1+\Omega_c^2}}{\sqrt{1+\Omega^2}}} \quad (23)$$

is always greater than one, for $\Omega<\Omega_c$. Thus, in effect, it takes more unit elements than LC elements to give a specified attenuation slope. A plot of R vs. Ω for several Ω_c values is given in Fig. 8. For increasing Ω_c, and for $(\Omega_c/2)<\Omega<\Omega_c$, the ratio approaches unity. This indicates that in the region immediately beyond cutoff for narrow to moderate bandwidth filters, a unit element gives almost the same attenuation characteristic as a stub-type element. However, as the filter bandwidth in-

creases, the unit element becomes less effective and more u.e.'s must be used to obtain the same attenuation as that of an LC element. The graph of Fig. 8 can be used to obtain a comparison of different m and n choices by letting

$$\frac{|\rho|^2}{|t|^2} = \epsilon^2 \cosh^2\left[m' \cosh^{-1}\frac{\Omega_c}{\Omega}\right] \tag{24}$$

and using the referenced nomographs, where

$$m' = m + \frac{n}{R}. \tag{25}$$

In practice, one estimates an average value of R from Fig. 8, obtains m' from (25), and finds the approximate network response from the appropriate nomograph in Kawakami [21]. A more accurate approximation can be obtained by using a new value of R for each Ω/Ω_c value investigated.

As an example consider the number of nonredundant elements $k=m+n=7$. Several choices of m and n are listed in Table IV along with an average m' for both a narrow-band and wide-band filter. For the narrow-band case, R is so close to unity that all forms give almost the same response. Thus, the choice of m and n is dictated by the practicality of a given network form. Stub network forms usually become unrealizable for narrow bandwidths, and coupled line structures, normally having a high value for n, are most practical. For example, the familiar parallel coupled filter employs $m=1$ and $n=k-1$, and is very practical to construct for narrow bandwidths.

For the wide-band case, the responses differ substantially for different choices of m and n and the networks containing more LC-type elements are observed to be superior. Referring to Table IV, the $m=3$ and $n=4$ case has a response corresponding to approximately 5.6 LC-type elements while the $m=0$, and $n=7$ case provides a characteristic similar to that of 4.5 LC elements. These approximations are only estimates for $(\Omega/\Omega_c > 0.6$. When Ω/Ω_c is less than 0.6, R becomes larger, resulting in a more degraded performance for those filters containing unit elements. However, most practical applications of wide-band microwave filters require steep skirt characteristics in which the behavior near cutoff is of greatest importance, and the above method of estimation is sufficient. The exact attenuation curve can be obtained from (8) and (22), if desired.

For wide-band filters, most choices of m and n result in prototypes that can be more easily realized with stub-type networks than with coupled line structures. The designer has the freedom of choosing m and n to meet specific size and performance requirements. Some unit elements are usually required, since only a limited number of stubs can be placed at a single junction. Thus,

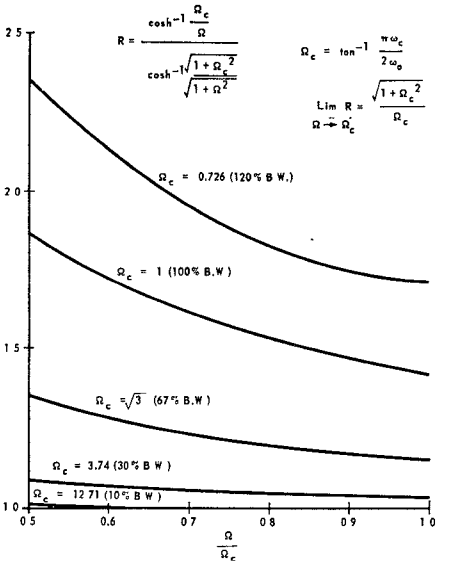

Fig. 8. Plot of R vs. Ω/Ω_c. Comparison of unit element and stub-type element attenuation properties for high-pass prototypes.

TABLE IV

PARAMETERS FOR COMPARISON OF DIFFERENT OPTIMUM MULTIPOLE FILTERS WITH $k=m+n=7$

10% BANDWIDTH			100% BANDWIDTH (3:1)		
m	n	$m' = m + \frac{n}{R}$	m	n	$m' = m + \frac{n}{R}$*
7	0	7	7	0	7
3	4	≈ 7	3	4	≈ 5.6
0	7	≈ 7	0	7	≈ 4.5

*R WAS CHOSEN TO BE 1.55

the $m=7$, and $n=0$ filter has the best response for all cases listed in Table IV, but a practical network would require the introduction of at least three redundant unit elements. The use of $m=7$ and $n=3$ would result in an improved filter by allowing the unit elements to contribute to the response. In the design example, a choice of $m=5$ and $n=2$ resulted in a response which is but slightly degraded from that of the case of $m=7$, $n=0$ in a structure only two thirds as long.

To obtain the best response from a filter of minimum size, the designer should try to incorporate as many LC elements as is practical. For wide-band designs the use of a high n/m ratio leads to a large network with a relatively poor response and should be avoided. In fact, in many cases, a low value of k with a low n/m ratio provides approximately the same attenuation as a high k value with a high n/m ratio. As an example, the response characteristic of a conventional filter constructed of shunt-shorted stubs placed a quarter wavelength apart is compared in Fig. 9 with the characteristic of the design example of Section V. The all-shunt-stub network form was designed using $m=1$ and $n=8$, and is four times longer than the $m=5$ and $n=2$ case, the latter of which exhibits a better response.

Redundant filter elements often must be incorporated to obtain practical element values. The redundancy can

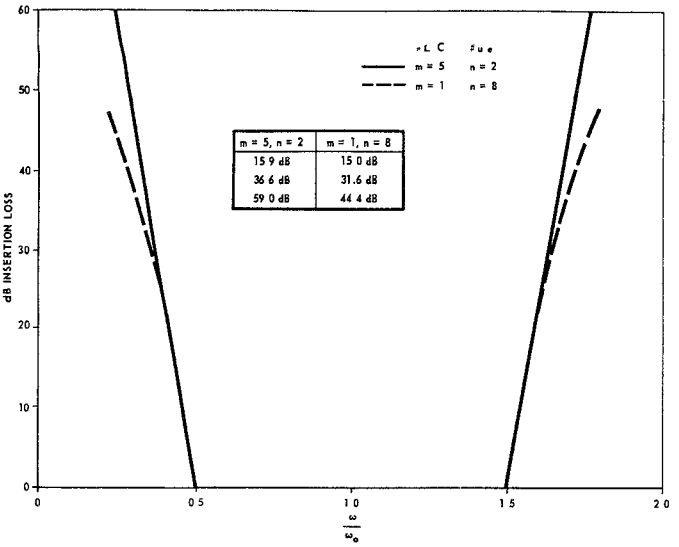

Fig. 9. Comparison of filter characteristics that demonstrates the size advantage obtained by using a low n/m ratio for wide-band designs.

either be added in the LC part of the network as in the design example, or in the unit element section [4], [12]. Redundant unit elements add length to the filter and thus it is more desirable to add the redundancy into the LC part of the network if possible. In wide-band designs it is usually most convenient to obtain the optimum multipole network and add redundant elements with the aid of Kuroda's Identities. For narrow-band designs, where redundancy is often high, it is more convenient to introduce redundant elements through the synthesis procedure.[8]

VII. Conclusions

The synthesis and design of a broad class of TEM mode filters has been presented in a three-step procedure. General transmission response functions were developed that give the "best" response (in a Butterworth or Chebyshev sense) for a given number of quarter-wave elements. A synthesis and design procedure was described that allows the realization of practical distributed networks in the form of quarter-wave lines. Direct application of the methods presented permits the exact design of most conventional TEM mode filter forms. By utilizing every quarter-wave element to augment the filter response, an optimum multipole filter can be obtained. A comparison of the filtering properties of stub-type elements with unit elements showed the stub types to be always superior and increasingly better for wider bandwidths. The unit element was shown to give effective band-pass filtering for bandwidths up to two octaves. The method of comparison presented can be used to determine the response characteristics of different optimum multipole network forms using bandwidth as a parameter. Comparisons of this type are useful in determining an optimum network form of minimum size. Use of the low-pass to high-pass transformation permits the band-pass results described to be applied to band-stop filters.

The procedures presented are also applicable to the design of certain types of waveguide filters for bandwidths of 20 per cent or less. These include those filter forms in which the response of the waveguide elements closely approximates that of TEM mode stub-type elements.

The basic approximating functions developed can also be used to design multiplexing filter networks by choosing the functions to represent squared magnitudes of the transfer admittances ($|Y_{12}|^2$) or transfer impedances ($|Z_{12}|^2$) and properly positioning the 3-dB cutoff frequencies [11]. Synthesis procedures applicable to obtaining a practical realization can be found in the literature [11], [13]–[15].

To verify the optimum multipole theory, a seven-section band-pass filter of 3 to 1 bandwidth was designed and constructed. The experimental results followed very closely those predicted by the theory.

VIII. Appendix

The equal ripple approximation to the ideal filter characteristic will be obtained by direct development from the definition of a constant amplitude rational fraction all-pass function on the complex W-plane.[9]

A unit amplitude all-pass transfer function on the imaginary axis in the complex W-plane is defined by:

$$e^{j2\phi_i(W)} = \frac{W_i + W}{W_i - W}. \tag{26}$$

The root parameter W_i must be real in order that (26) be a rational unit amplitude function describing the transfer characteristic of a realizable filter. However, if a product of such functions is taken, the resulting unit amplitude function will be rational if the W_i's are either real or occur in conjugate pairs. Thus a rational unit amplitude transfer function on the imaginary axis in W can be represented by the product,

$$e^{j2\phi(W)} = \Pi e^{j2\phi_i(W)} = \frac{\Pi(W_i + W)}{\Pi(W_i - W)} \tag{27}$$

[8] As described, for example, in Wenzel [4], pp 109–110.

[9] A similar approach has been used by Bennett [22], [23] for application to RC lumped element networks and leads to the desired equal ripple approximation via relatively simple logic. The rational fraction functions used by Sharpe [24] and Helman [25], [26] for lumped RC networks are also applicable but no justification is given for their choice. Kohler and Carlin [27] go through a lengthy justification after having chosen the proper approximation for the distributed optimum low-pass filter. Perhaps the earliest discovery of the proper equal ripple approximating function for the distributed optimum filter was recorded in a personal letter from Prof. Kuroda to Prof. Ozaki in 1954, reference to which was found in unpublished notes written by Prof. Fujisawa while a visiting lecturer at the University of Michigan in 1963.

where the symbol Π indicates the product taken over all roots W_i which must occur in conjugate pairs if not real. The magnitude of $e^{j2\phi(W)}$ is unity on the imaginary axis in W and the phase variation is monotonic. Similarly, the positive square root of (27) is of constant unit amplitude,

$$e^{j\phi} = \Pi e^{j\phi_i} = e^{j\Sigma\phi_i} = \frac{\Pi\sqrt{W_i + W}}{\Pi\sqrt{W_i - W}} \tag{28}$$

with the symbol Σ indicating summation on all angles ϕ_i associated with roots W_i. A real function $f(W)$ is defined by

$$f(W) = \tfrac{1}{2}(e^{j\phi} + e^{-j\phi}) = \cos\phi = \cos\Sigma\phi_i. \tag{29}$$

This function has a maximum amplitude of unity and is the cosine of a monotonic varying angle ϕ along the imaginary axis in W. Using (28) in (29),

$$f(W) = \frac{\Pi(W_i + W) + \Pi(W_i - W)}{2\Pi\sqrt{W_i^2 - W^2}} \tag{30}$$

which is equal ripple along the entire imaginary axis in the W-plane.

A. High Pass

Equal ripple variation may be restricted to the high-pass range on the imaginary S-plane axis $S > S_c$ by applying to (30) the transformation:

$$W = \sqrt{1 - S^2/S_c^2}; \qquad W_i = \sqrt{1 - S_i^2/S_c^2}. \tag{31}$$

This transform maps that portion of the positive imaginary S-plane axis for which $S > S_c$ onto the entire positive imaginary W-plane axis, as shown in Fig. 10. The remainder of the positive imaginary S-plane axis $S < S_c$ maps onto the positive real axis in the W-plane between unity and zero.

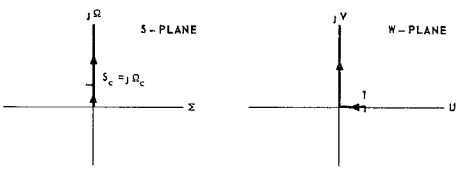

Fig. 10. Mapping of the positive imaginary S-plane axis onto the W-plane by the high-pass transformation $W = \sqrt{1 - S^2/S_c^2}$.

The high-pass equal ripple function $F_H(S) = f(W)$ is obtained by substituting transformation (31) into (30) to give:

$$F_H(S) = \frac{\Pi(\sqrt{S_i^2 - S_c^2} + \sqrt{S^2 - S_c^2}) + \Pi(\sqrt{S_i^2 - S_c^2} - \sqrt{S^2 - S_c^2})}{2\Pi\sqrt{S_i^2 - S^2}}. \tag{32}$$

The roots S_i in (32) may be chosen arbitrarily as long as they occur in conjugate pairs if not real. It is noted that the real roots $S_i = 0$ and $S_i = -1$ permit the square of F_H in (32) to have the same pole locations as those of $|\rho|^2/|t|^2$ in (9). If the pole locations of F_H are now restricted such that m poles occur at $S_i = 0$, corresponding to m high-pass LC ladder elements, and n poles occur at $S_i = -1$, corresponding to n. u.e.'s, then (32) for the optimum multipole equal ripple filter becomes

$$F_H(S) = \frac{(jS_c + \sqrt{S^2 - S_c^2})^m(\sqrt{1 - S_c^2} + \sqrt{S^2 - S_c^2})^n + (jS_c - \sqrt{S^2 - S_c^2})^m(\sqrt{1 - S_c^2} - \sqrt{S^2 - S_c^2})^n}{2(jS)^m(\sqrt{1 - S^2})^n}. \tag{33}$$

This algebraic fraction, representing a unit amplitude optimum equal ripple approximation, can be expressed alternately in Chebyshev polynomials by noting that $F(S) = f(W) = \cos\phi = \cos\Sigma\phi_i$ in (29). Thus the ith component phase angle ϕ_i is obtained by considering only the ith term from each of the products in (32) for F_H:

$$\cos\phi_i = \frac{\sqrt{S_i^2 - S_c^2}}{\sqrt{S_i^2 - S^2}}. \tag{34}$$

The high-pass LC ladder element phase angle ϕ_{LC} is established by setting $S_i = 0$; similarly, the u.e. phase angle $\phi_{\text{u.e.}}$ is established by setting $S_i = -1$, yielding

$$\cos\phi_{LC} = \frac{jS_c}{jS} = \frac{\tan\theta_c}{\tan\theta};$$

$$\cos\phi_{\text{u.e.}} = \frac{\sqrt{1 - S_c^2}}{\sqrt{1 - S^2}} = \frac{\cos\theta}{\cos\theta_c}. \tag{35}$$

From (29) the high-pass approximating function F_H may be written alternately as

$$F_H = \cos(m\phi_{LC} + n\phi_{\text{u.e.}})$$

$$F_H = T_m\left(\frac{\tan\theta_c}{\tan\theta}\right) T_n\left(\frac{\cos\theta}{\cos\theta_c}\right) - U_m\left(\frac{\tan\theta_c}{\tan\theta}\right) U_n\left(\frac{\cos\theta}{\cos\theta_c}\right) \tag{36}$$

where $T_m(x) = \cos(m \arccos x)$ and $U_m(x) = \sin(m \arccos x)$ are un-normalized mth degree Chebyshev polynominals of the first and second kinds, respectively [19].

B. Low Pass

A low-pass approximating function F_L can be obtained from the high-pass function F_H by replacing each frequency parameter by its inverse. Thus, (35), (33), and (36) become now, for the low-pass case,

$$\cos \phi_{LC} = \frac{S}{S_c} = \frac{\tan \theta}{\tan \theta_c}; \quad \cos \phi_{\text{u.e.}} = \frac{S\sqrt{1 - S_c^2}}{S_c\sqrt{1 - S^2}} = \frac{\sin \theta}{\sin \theta_c} \tag{37}$$

$$F_L = \frac{(S + \sqrt{S^2 - S_c^2})^m(S\sqrt{1 - S_c^2} + \sqrt{S^2 - S_c^2})^n + (S - \sqrt{S^2 - S_c^2})^m(S\sqrt{1 - S_c^2} - \sqrt{S^2 - S_c^2})^n}{2(S_c)^{m+n}(\sqrt{1 - S^2})^n} \tag{38}$$

$$F_L = \cos (m\phi_{LC} + n\phi_{\text{u.e.}})$$

$$F_L = T_m\left(\frac{\tan \theta}{\tan \theta_c}\right) T_n\left(\frac{\sin \theta}{\sin \theta_c}\right) - U_m\left(\frac{\tan \theta}{\tan \theta_c}\right) U_n\left(\frac{\sin \theta}{\sin \theta_c}\right). \tag{39}$$

The functions F_H and F_L exhibit equal ripple characteristics and monotonic phase variation in their respective pass bands and have pole locations corresponding to the R-matrix multiplication of unit elements and LC ladder elements. The unit amplitude equal ripple functions, F_H of (33) or (36) and F_L of (38) or (39), are each multiplied by an arbitrary voltage ripple factor ϵ and then squared in order to form the Chebyshev approximation to the power reflection-to-transmission ratio.

$$\text{H-P:} \quad \frac{|\rho|^2}{|t|^2} = \epsilon^2 F_H{}^2$$

$$\text{L-P:} \quad \frac{|\rho|^2}{|t|^2} = \epsilon^2 F_L{}^2. \tag{40}$$

Acknowledgment

The authors wish to thank Dr. W. G. Jaeckle and P. C. Goodman for their discussions and valuable suggestions during the course of this work. Acknowledgment is also due T. E. Gordon, who constructed the experimental filter and carried out the measurements.

References

[1] Cohn, S. B., Parallel-coupled transmission-line-resonator filters, *IRE Trans. on Microwave Theory and Techniques*, vol MTT-6, Apr 1958, pp 223–231.

[2] Matthaei, G. L., et al., Design criteria for microwave filters and coupling structures, Final Rept, SRI Project 2326, Contract DA36-039SC7-4862, Stanford Research Inst,. Menlo Park, Calif., Jan 1961.

[3] Matthaei, G. L., Design of wide-band (and narrow-band) bandpass microwave filters on the insertion loss basis, *IRE Trans. on Microwave Theory and Techniques*, vol MTT-8, Nov 1960, pp 580–593.

[4] Wenzel, R. J., Exact design of TEM microwave networks using quarter-wave lines, *IEEE Trans. on Microwave Theory and Techniques*, vol MTT-12, Jan 1964, pp 94–111.

[5] Ozaki, H., and J. Ishii, Synthesis of transmission-line networks and the design of UHF filters, *IRE Trans. on Circuit Theory*, vol CT-2, Dec 1955, pp 325–336.

[6] ——, Synthesis of a class of strip-line filters, *IRE Trans. on Circuit Theory*, vol CT-5, Jun 1958, pp 104–109.

[7] Jones, E. M. T., Synthesis of wide-band microwave filters to have prescribed insertion loss, *1956 IRE Conv. Rec.*, pt 5, pp 119–128.

[8] Grayzel, A. I., A synthesis procedure for transmission line networks, *IRE Trans. on Circuit Theory*, vol CT-5, Sep 1958, pp 172–181.

[9] Horton, M. C., and R. J. Wenzel, Exact design of filters by network techniques, *Microwaves*, vol 3, Apr 1964, pp 16–21.

[10] Wenzel, R. J., Summary of methods for practical synthesis of distributed filter networks, in *Symp. Digest, 7th Midwest Symp. on Circuit Theory*, University of Michigan, Ann Arbor, Mich., May 1964.

[11] Wenzel, R. J., Application of exact synthesis methods to multichannel filter design, *IEEE Trans. on Microwave Theory and Techniques*, vol MTT-13, Jan 1965, pp 5–15.

[12] Schiffman, B. M., and G. L. Matthaei, Exact design of bandstop microwave filters, *IEEE Trans. on Microwave Theory and Techniques*, vol MTT-12, Jan 1964, pp 6–15.

[13] Guillemin, E. A., *Synthesis of Passive Networks*. New York: Wiley, 1957.

[14] Weinberg, L., *Network Analysis and Synthesis*. New York: McGraw-Hill, 1962.

[15] Balabanian, N., *Network Synthesis*. Englewood Cliffs, N. J.: Prentice-Hall, 1958.

[16] Richards, P. I., Resistor-transmission-line circuits, *Proc. IRE*, vol 36, Feb 1948, pp 217–220.

[17] Kuroda, K., Derivation methods of distributed constant filters from lumped constant filters, text for lectures at Joint Meeting of Konsoi Branch of Institute for Elec. Commun., of Elec., and of Illumin. Engrs. of Japan, Oct 1952, p 32 (in Japanese).

[18] Beatty, R. W., and D. M. Kerns, Relationships between different kinds of network parameters, not assuming reciprocity or equality of the waveguide or transmission line characteristic impedances, *Proc. IEEE (Correspondence)*, vol 52, Jan 1964, p 84.

[19] Clement, P. R., The Chebyshev approximation method, *Quart. appl. Math.*, vol 11, Jul 1953, pp 167–183.

[20] *The Microwave Engineers Handbook*. Brookline, Mass.: Horizon House-Microwave, Inc., 1963.

[21] Kawakami, M., Nomographs for Butterworth and Chebyshev filters, *IEEE Trans. on Circuit Theory*, vol CT-10, Jun 1963, pp 288–289.

[22] Bennett, B. J., Synthesis of electric filters with arbitrary phase characteristics, *1953 IRE Conv. Rec.*, pt 5, pp 19–26.

[23] ——, Rebuttal, *IRE Trans. on Circuit Theory (Correspondence)*, vol CT-2, Jun 1955, p 218.

[24] Sharpe, C. B., A general Chebyshev rational function, *Proc. IRE*, vol 42, Feb 1954, pp 454–457.

[25] Helman, D., Chebyshev approximations for amplitude and delay with rational functions, *Proc. of the Symp. on Modern Network Synthesis*, Apr 1955, pp 385–402.

[26] ——, Synthesis of electric filters with arbitrary phase characteristics, *IRE Trans. on Circuit Theory (Correspondence)*, vol CT-2, Jun 1955, pp 217–218.

[27] Kohler, W., and H. J. Carlin, Equiripple transmission line networks, Rept PIB MRI-1089-62, Microwave Research Instit., Polytechnic Institute of Brooklyn, New York, Jan 1963.